Desalination and Water Treatment
www.deswater.com

doi: 10.1080/19443994.2016.1152645

57 (2016) 24557–24565
November

Taylor & Francis
Taylor & Francis Group

Influence of microbial floatation on membrane fouling due to particles and organic matters in submerged microfiltration

O.G. Manvoudou Pissibanganga[a], Jungwoo Jung[b], Yongjun Choi[a], Sangho Lee[a,*], Jinsik Sohn[a], Namjun Cho[a]

[a]*School of Civil and Environmental Engineering, Kookmin University, Seoul, Korea, Tel. +82 2 910 5060; Fax: +82 2 910 8597; emails: deliapish@gmail.com (O.G. Manvoudou Pissibanganga), choiyj1041@gmail.com (Y. Choi), Tel. +82 2 910 4529; Fax: +82 2 910 8597; email: sanghlee@kookmin.ac.kr (S. Lee), Tel. +82 2 910 4528; Fax: +82 2 910 4939; email: jinsiksohn@kookmin.ac.kr (J. Sohn), Tel. +82 2 910 4699; Fax: +82 2 910 4939; email: njcho@kookmin.ac.kr (N. Cho)*
[b]*Hyorim Industries Inc., Yatap-don, Bundang-gug, Seongnam-city, Gyeonggi-do, Tel. +82 10 3126 4478; Fax: +82 53 781 3779; email: jungjw@hyorim.co.kr*

Received 23 October 2015; Accepted 8 January 2016

ABSTRACT

This study investigated the effect of microbubble floatation on the fouling of microfiltration membranes. Synthetic feed solutions containing either kaolin or alginic acid were used for the membrane filtration tests. A dissolve air flotation system using a pump-type microbubble generator was adopted as a pretreatment for microfiltration system. A multi-array submerged membrane filtration system was used to monitor the changes in transmembrane pressure with time under various operating conditions. Turbidity removal efficiency, particle counts, and fouling rate for the microfiltration membrane were measured after the microfiltration floatation. The effect of coagulant dose on the treated water quality and membrane performance was also investigated. Results showed that microbubble floatation without coagulant was effective to reduce membrane fouling by kaolin but it was not very effective to control fouling by alginate. With the aid of coagulant, microbubble flotation could control fouling by alginate. This is attributed to the removal mechanisms of foulants by microbubble floatation: suspended particles can be separated by the microbubbles without coagulant but dissolved organics can be only removed by the combined effect of coagulation and floatation.

Keywords: Microbubble; Flotation; Microfiltration; Fouling; Coagulation; Pretreatment

1. Introduction

Dissolved air flotation (DAF) is one of the advanced water treatment techniques, aiming at the removal of pollutants for the clarification of water and wastewater [1–3]. This can be done by pressurizing air into water and releasing it in a flotation tank or basin, which forms small air bubbles [4]. Pollutants such as suspended particles, oils, and greases can be adsorbed on the surface of the bubble and separated as a form

*Corresponding author.

Presented at 2015 Academic Workshop for Desalination Technology held in the Institute for Far Eastern Studies Seoul, Korea, 23 October 2015

of scum on the surface of water. This is widely accepted for the treatment of municipal and industrial wastewaters [2,5,6].

The efficiency of DAF can be improved by adjusting the properties of bubbles used for pollutant removal [7]. One of such approaches is microbubble floatation [8]. Microbubbles are defined as bubbles with diameters on the order of 10–50 μm and have unique properties due to their small size [8,9]. For instance, microbubbles have high-specific surface area (the ratio of surface area to the volume), allowing the high efficiency of pollutant adhesion [7,10]. Due to its high effectiveness of pollutant removal, microbubble floatation has drawn attention for not only wastewater treatment [11–13] but also water purification [14,15] and pretreatment for seawater desalination [16–18].

One of the possibilities of using microbubble floatation is the pretreatment of feedwater to membrane process. Microfiltration (MF) and ultrafiltration (UF) are increasingly used although fouling of these membranes is still a serious issue [19–21]. Currently, coagulation is applied for the pretreatment of feedwater to MF/UF process [22–28]. However, it is difficult to remove particles with low density and organic matters by this technique. Accordingly, the application of microbubble floatation prior to MF or UF may have potential to control fouling by low-density particles, organic matters, and algae. Nevertheless, there are relatively few fundamental research works on the application of microbubble floatation as a pretreatment for MF or UF membranes. In addition, optimum conditions for microbubble floatation process are not fully revealed yet. Accordingly, this study focused on the investigation of the effect of microbubble floatation on the fouling of microfiltration membranes. Using synthetic feedwaters containing model foulants, the fundamental properties of microbubble floatation were experimentally examined. Moreover, the effect of coagulant dose on the pretreatment efficiency by microbubble floatation was also explored.

2. Materials and methods

2.1. Feed solutions

Two different synthetic feed solutions were prepared for the experiments of microbubble floatation and microfiltration. The first synthetic solution contained kaolin of 150 mg/L and the second one contained sodium salt of alginic acid of 150 mg/L. Prior to the experiments, either kaolin or alginate was added to the deionized water of 40 L. All the solutions were mixed by an electromagnetic stirrer for 1 h. After the stirring, each solution was transferred into the flotation device or into the MF system. All experiments were carried out at room temperature (25˚C). Table 1 shows the water quality parameters of the synthetic feedwaters.

2.2. Experimental setup

Fig. 1 shows the schematic diagram for the microbubble floatation device. This system consists of a feed tank, a microbubble generator, and a floatation tank. The feed and floatation tanks are made of acrylic resin. The microbubble generator used a three phase induction motor (KTM15N1D042 M-000, Toshiba, Japan). The water flow rate was 8 L/min and the gas flow rate was 0.64 L/min. Microbubbles were produced using a gas–water circulation type generator, and supplied to the bottom of the tank under the pressure of 4 bar. According the manufacturer, the average size of the microbubbles was 40 μm. The flotation was operated in a continuous flow mode for 5 min. Water samples were taken at 0, 2.5, and 5 min of flotation. Therefore, three samples were obtained for each test.

This microbubble floatation system was operated without and with adding coagulant. Poly aluminum chloride (PACl) was used as the coagulant. The dose of PACl was determined to be 2 mg/L based on the Jar test results. To examine the effect of coagulation on the efficiency of microbubble floatation, PACl was directly added to the feed tank of the microbubble floatation system.

After the microbubble floatation, microfiltration experiments were carried out using a multi-array membrane filtration system. The detailed information on this system is available elsewhere [29]. The experiments were conducted using hollow fiber membranes made of polyvinylidene fluoride. Prior to the filtration test, the membrane fibers were immerged into ethanol solution for 1 h and then rinsed with deionized water for pore wetting. Then, the membranes were vertically submerged into a cylindrical feed tank. In each feed tank, a magnetic stirrer was placed for continuous mixing of solution. The pure water flux was measured using deionized water and then the permeate flux was measured using the feedwater pretreated by microbubble floatation. A multi-channel cartridge

Table 1
Water quality parameters of the synthetic feedwaters

	Turbidity (NTU)	pH
Kaolin solution	110–125	5.5
Alginate solution	50–70	5

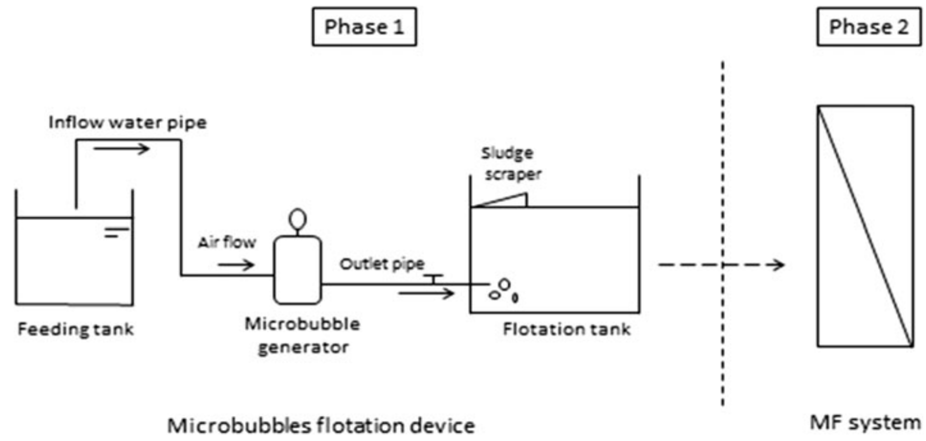

Fig. 1. Schematic diagram for the microbubble floatation device.

peristaltic pump (model 7535-08, Cole Palmer, USA) was used, which allows up to 15 filtration tests at the same time. A pressure transducer monitored the transmembrane pressure through the membrane under constant flux mode. The filtration tests were done at three different flux conditions: 30, 60, and 90 L/m^2 h. All the data were collected by a data logger and recorded by a data acquisition software. The test conditions for the membrane filtration are summarized in Table 2.

2.3. Calculation of fouling rate

Using the results on transmembrane pressure, fouling rate was calculated using the following method. To begin, a simple filtration model to estimate the fouling rates in dead-end filtration system was applied. Assuming that fouling occurs through cake formation mechanisms, the transmembrane pressure is given by [30,31]:

Table 2
Conditions for microfiltration experiments using hollow fiber membranes

Parameters	Conditions
Membrane material	PVDF (polyvinylidene difluoride)
Pore size	0.1 μm
Fiber diameter	O.D 1.15/ID 0.7 mm
Length	240 mm
Flow configuration	Outside-In
Type of treatment	Dead-end filtration
Flux	30, 60, 90 L/m^2 h for 2 h at each flux
Temperature	25℃

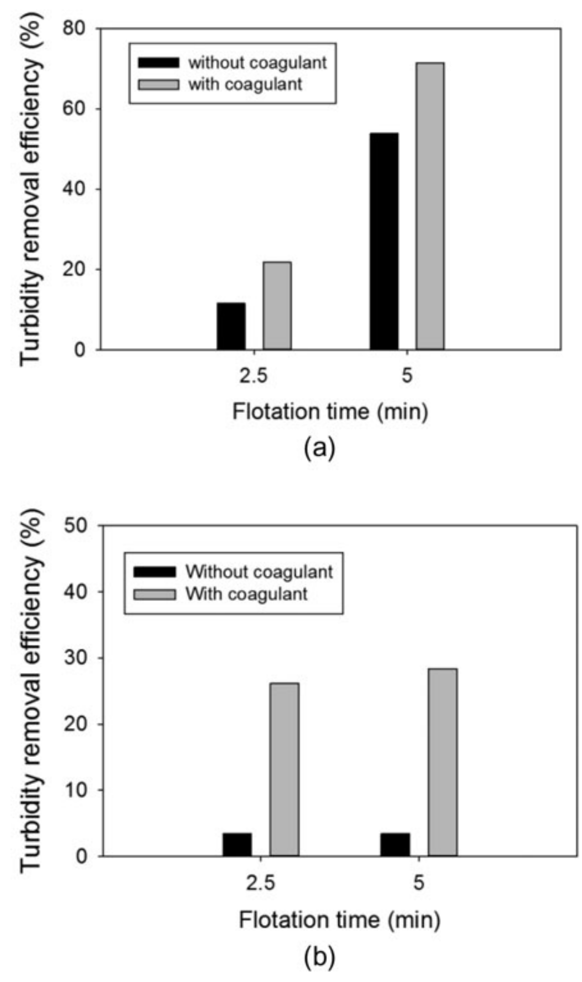

Fig. 2. Effect of microbubble flotation on turbidity removal with and without using PACl: (a) kaolin solution and (b) alginate solution.

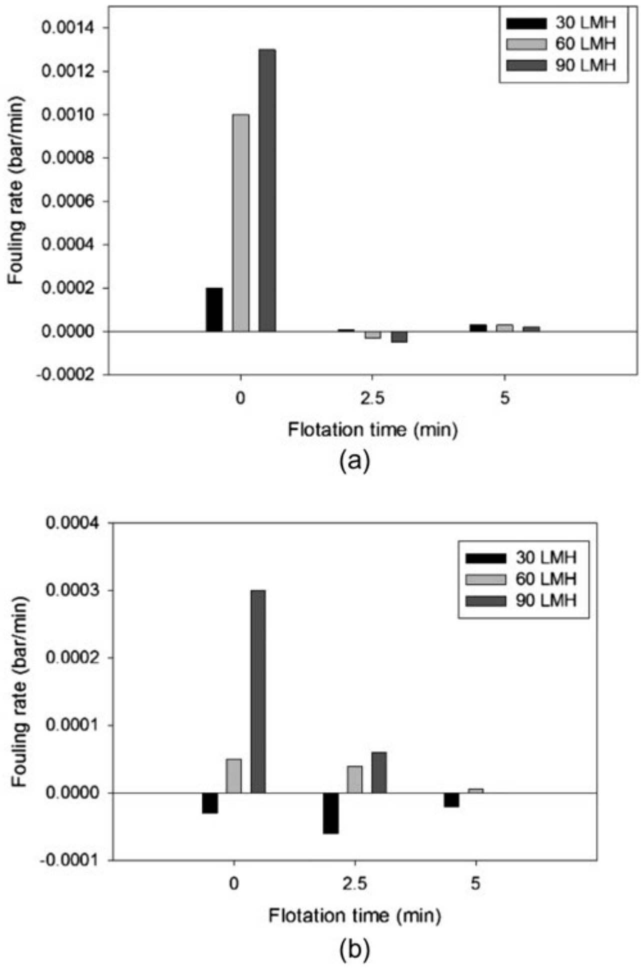

Fig. 3. Dependence of fouling rate on floatation time at different flux conditions for kaolin solution. (a) Microbubble floatation without PACl and (b) Microbubble floatation with PACl (2 mg/L).

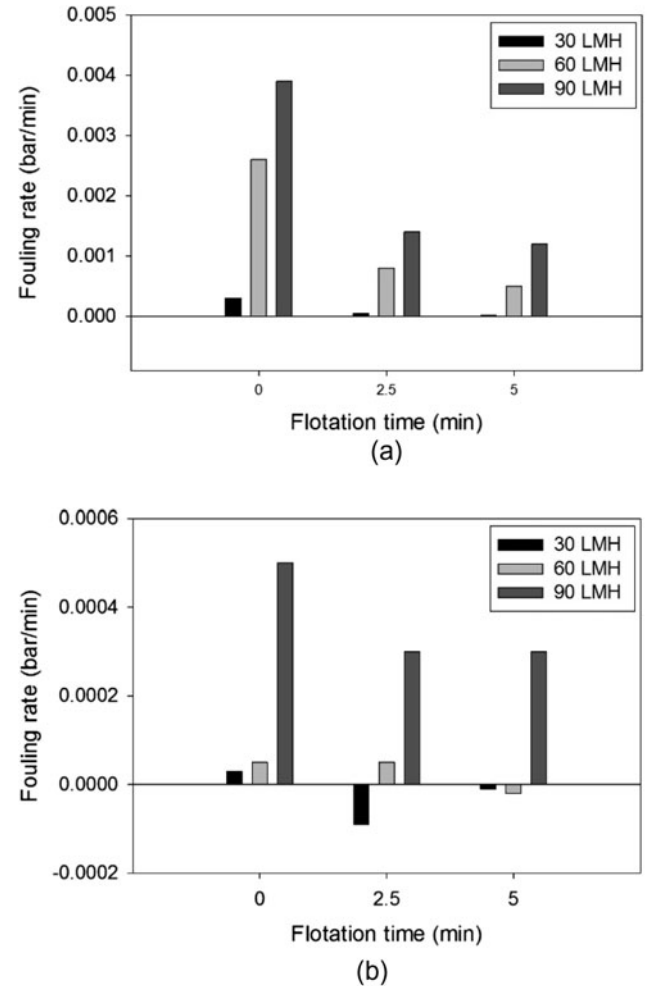

Fig. 4. Dependence of fouling rate on floatation time at different flux conditions for alginate solution: (a) Microbubble floatation without PACl and (b) Microbubble floatation with PACl (2 mg/L).

$$\Delta P = \mu(R_m + R_c)J \tag{1}$$

where J is the permeate flux, ΔP is the transmembrane pressure, μ is the absolute viscosity of water, R_m is the intrinsic membrane resistance, and R_c is the cake resistance. The cake resistance is a function of the specific cake resistance (α), the mass of the cake deposited on the membrane (m_c), and the membrane area (A_m) [32]:

$$R_c = \frac{\alpha\, m_c}{A_m} \tag{2}$$

Since the dead-end filtration was assumed, the cake mass m_c is given by:

$$m_c = J\, A_m c\, t \tag{3}$$

where c is the effective concentration of the foulant. By combining the Eqs. (1)–(3), ΔP is given by [33]:

$$\Delta P = \mu\, R_m J + \mu\, \alpha\, c\, J^2 t = \mu\, J\, R_m + \theta\, t \tag{4}$$

where θ is defined as the fouling rate. In a constant flux operation, θ can be calculated from the slope of t and ΔP:

$$\theta = \frac{d\Delta P}{dt} = \alpha\, \mu\, J^2\, c \tag{5}$$

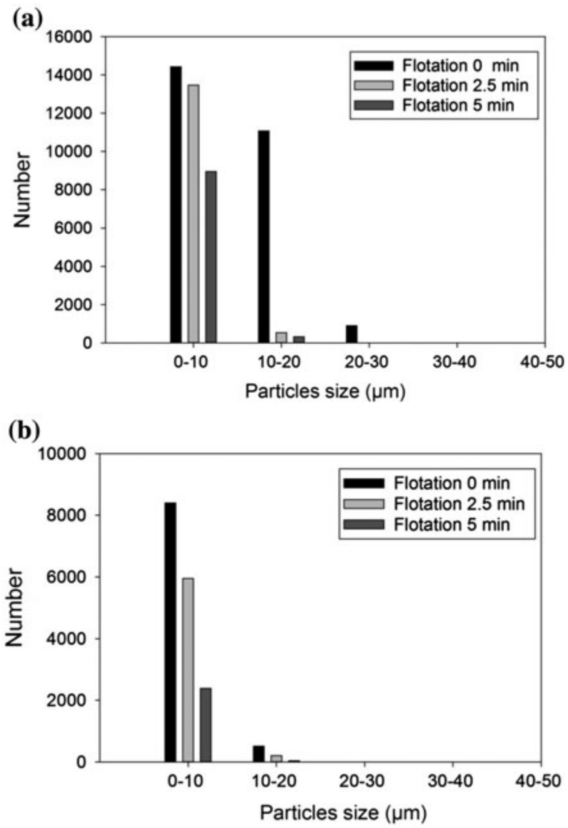

Fig. 5. Effect of microbubble floatation on particle counts for kaolin solution: (a) without PACl (b) with PACl.

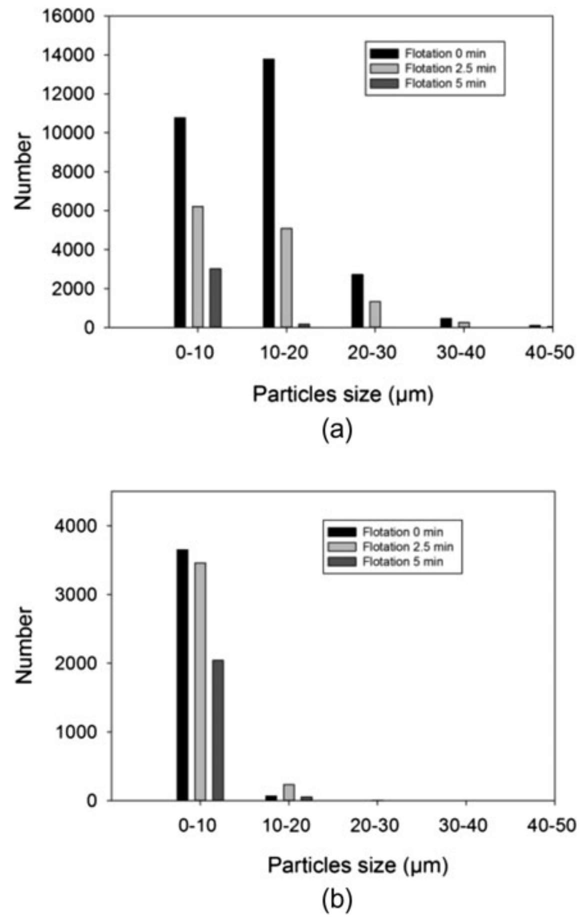

Fig. 6. Effect of microbubble floatation on particle counts for alginate solution: (a) without PACl (b) with PACl.

Accordingly, θ is proportional to the product of the specific cake resistance and effective concentration of foulants, which represents the potential of fouling for the feedwater. Moreover, θ is also proportional to the J^2, implying that fouling is accelerated at high flux rate.

2.4. Analytical methods

Turbidity and pH of the water sample were measured using a turbidity meter (TURIB 430 IR, Germany) and a pH meter (Orion Star, Thermo Scientific), respectively. The distribution of particles in the water samples was analyzed using a particle counter (CHEMTRAC laser trac particle counter PC 3400, USA). After the microfiltration tests, the surface of the membrane and foulant layer were examined by Field emission scanning electron microscopy (Model: S-4700, Hitachi, Japan).

3. Results and discussion

3.1. Effect of microbubble floatation on turbidity removal

As listed in Table 1, the turbidity values for the kaolin and alginate solutions were in the range between 110 and 125 NTU and between 50 and 70 NTU, respectively. After microbubble floatation, the turbidity of the feed solutions was changed. Fig. 2(a) shows the turbidity removal efficiency for the kaolin solution by microbubble floatation. At the floatation time of 2.5 min, the turbidity removal was less than 20%. However, the turbidity removal increased with increasing the floatation time up to 5 min. With the addition of PACl, the turbidity removal was higher (~72%) than that without using PACl (~57%).

However, the turbidity removal for the alginate solution was different from that for the kaolin solution. Without using PACl, the turbidity removal was less than 5%, implying that the removal efficiency is very low. The turbidity removal increased up to 29%

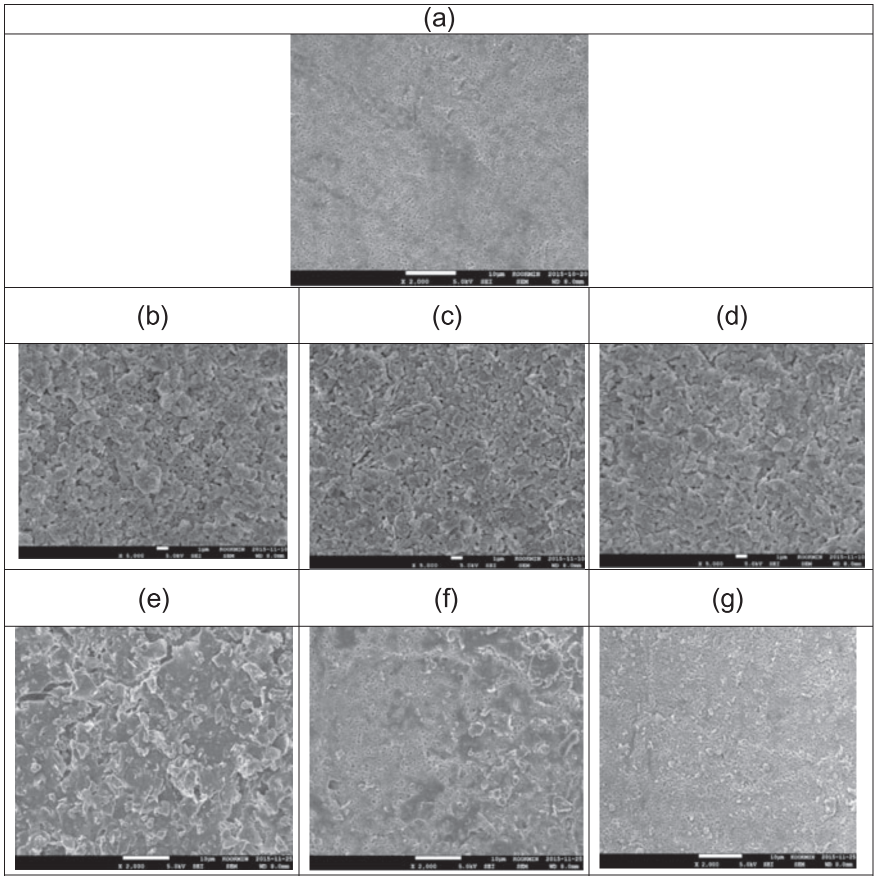

Fig. 7. SEM images of membrane surfaces after microfiltration experiments using the kaolin solution: (a) clean membrane, (b) control, (c) microbubble floatation (2.5 min), (d) microbubble floatation (5 min), (e) control with PACl, (f) microbubble floatation with PACl (2.5 min), and (g) microbubble floatation with PACl (5 min).

by adding PACl but it is still a low value. Since particulate forms of alginate result in turbidity in this feed solution, it is difficult to reduce turbidity by removing alginate by coagulation and air floatation. Accordingly, the turbidity removal in the alginate solution should be lower than that in the kaolin solution. These results suggest that microbubble floatation is effective to remove particulate matters but is not efficient to remove organic particles without added coagulant.

3.2. *Effect of microbubble floatation on MF fouling rate*

Fig. 3(a) compares the fouling rates (θ) at different floation time and flux values for the kaolin solution. In this case, microbubble floatation was applied without PACl addition. Before applying microbubble floatation, the fouling rate was high. As the flux increased, the fouling rate increased, which is evident from Eq. (5). After applying micrbubble floatation, the fouling rate became negligible, implying that the fouling by kaolin was efficiently reduced even without using coagulant.

The fouling rates of the kaolin solution treated by microbubble floatation with PACl were shown in Fig. 3(b). At the flotation time of 0 min, PACl was added to the feed solution and no microbubble floatation was applied. Nevertheless, the fouling rates were reduced by the effect of coagulation by the added PACl. After applying the microbubble, the fouling rates were further reduced. Again, the fouling by kaolin could be alleviated by microbubble floatation and PACl.

Fig. 4 shows the effect of microbubble floatation on the fouling rate of the alginate solution. Without PACl addition (Fig. 4(a)), the microbubble floatation was less efficient to decrease fouling rate for the alginate solution than for the kaolin solution. This could be attributed to low removal of turbidity by the microbubble floatation without PACl as shown in Fig. 2(b). Nevertheless, the microbubble floatation

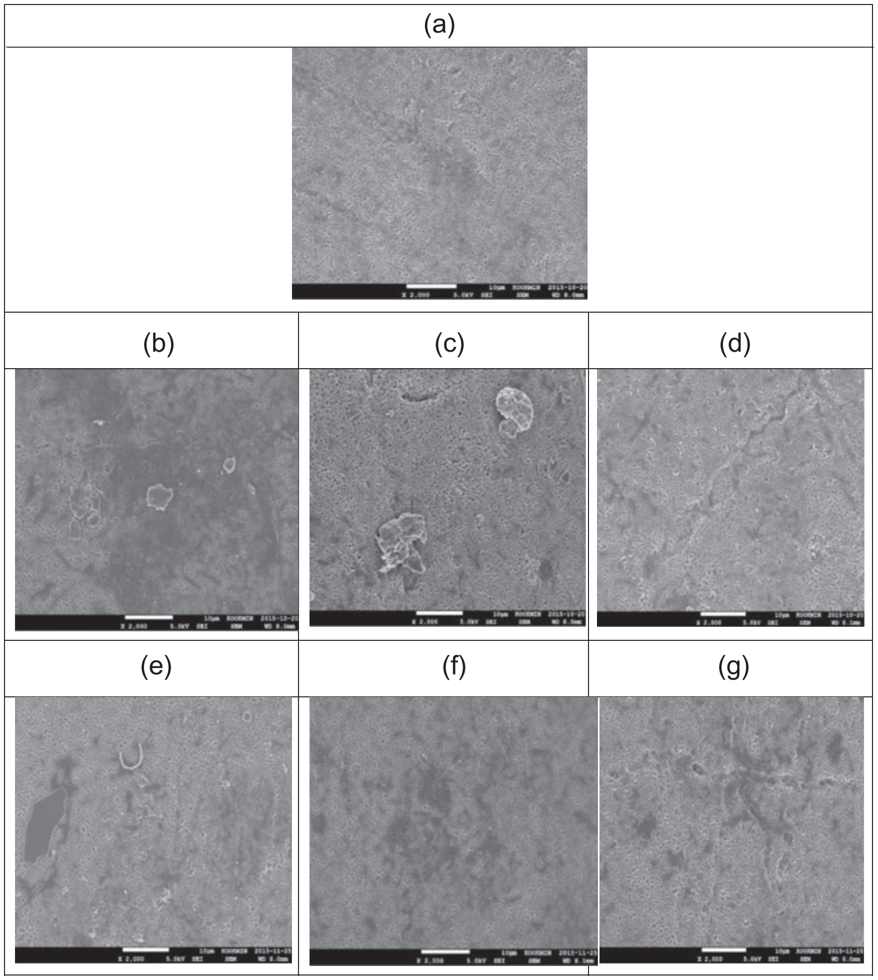

Fig. 8. SEM images of membrane surfaces after microfiltration experiments using the alginate solution: (a) clean membrane, (b) control, (c) microbubble floatation (2.5 min), (d) microbubble floatation (5 min), (e) control with PACl, (f) microbubble floatation with PACl (2.5 min), and (g) microbubble floatation with PACl (5 min).

could reduce the fouling rate by more than 50%. When PACl was used in the microbubble floatation, the fouling rate was significantly reduced as shown in Fig. 4(b). This suggests that the fouling by alginate could be efficiently reduced by the combination of microbubble floatation and PACl addition.

3.3. Changes in particle counts by microbubble floatation

The results on the particle size analysis are shown in Figs. 5 and 6. The information on the particle size distribution in the feed solution to MF/UF is important for better understanding of the fouling potential. Although similar amounts of particles exist, the smaller particles cause more severe membrane fouling than the larger ones. As shown in Fig. 5(a), the total number of particles was decreased by applying microbubble floatation. Especially, the particles in the range between 10 and 20 μm were removed after microbubble floatation of 2.5 min. The particles in the range between 0 and 10 μm were also removed after microbubble floatation of 5 min. With the addition of PACl, the particles were further removed by microbubble floatation. The total number of particles in the range between 0 and 50 μm was reduced to 2,500 per mL after microbubble floatation of 5 min with PACl.

Fig. 6 shows the particle size distribution for the alginate solution with microbubble floatation. Without PACl, the number of particles was reduced by the microbubble floatation but the efficiency was relatively low. With the addition of PAC, the number of particles significantly decreased by the microbubble floatation. Again, it was confirmed that microbubble floatation together with PACl addition is required to reduce fouling potential for the alginate solution.

3.4. SEM analysis of foulant layers on the membrane

After the microfiltration tests, the membrane was stored and prepared for the SEM analysis to visualize the changes in foulant layer by microbubble floatation. Fig. 7 shows the SEM images of the membrane surface after microfiltration of the kaolin solution. It appears that the foulant layer on the membrane surface is affected by the feedwater pretreatment using microbubble floatation. For example, a thick layer of the cake was observed in Fig. 7(e) (control with PACl), while a thin and porous cake layer was found in Fig. 7(f) and (g). This suggests that the microbubble floatation changed the morphology of the cake layer. Similar results were found with the alginate solution as shown in Fig. 8(b)–(d).

4. Conclusions

In this study, the effect of microbubble floatation on the fouling of microfiltration membranes was investigated. The following conclusions were withdrawn:

(1) Microbubble floatation without PACl was found to be effective to remove turbidity from the kaolin feed solution. However, it was not efficient to remove turbidity from the alginate feed solution. In this case, the removal efficiency of the turbidity was improved by the addition of PACl (2 mg/L) to the microbubble floatation tank.
(2) The fouling rate of the kaolin feed solution was reduced by microbubble floatation without PACl addition. A further decrease in the fouling rate was also observed with PACl addition.
(3) The fouling rate of the alginate feed solution was not effectively reduced by microbubble floatation alone. In this case, PACl addition was required to reduce the fouling rate.
(4) Microbubble floatation affected the particle counts of the feed solutions. It took more time to remove smaller particles without PACl addition.
(5) The analysis of SEM images suggests that the morphology of the fouling layer changes by microbubble floatation. More porous cake layer could be formed after the pretreatment of feedwater using the microbubble floatation.

Acknowledgment

This research was supported by the Korea Ministry of Environment as "The Eco-Innovation project (Global Top project)". (GT-SWS-11-02-007-9).

List of abbreviations

A_m	—	membrane area
c	—	effective foulant concentration
DAF	—	dissolved air flotation
J	—	flux
LMH	—	liters per square meter per hour ($L/m^2/h$)
m_c	—	mass of the cake
MF	—	microfiltration
R_m	—	clean membrane resistance
R_c	—	cake resistance
TMP	—	transmembrane pressure
μ	—	absolute viscosity
ΔP	—	transmembrane pressure
θ	—	fouling rate

References

[1] M.N. Adlan, P. Palaniandy, H.A. Aziz, Optimization of coagulation and dissolved air flotation (DAF) treatment of semi-aerobic landfill leachate using response surface methodology (RSM), Desalination 277(1–3) (2011) 74–82.
[2] P. Palaniandy, M.N. Adlan, H.A. Aziz, M.F. Murshed, Application of dissolved air flotation (DAF) in semi-aerobic leachate treatment, Chem. Eng. J. 157(2–3) (2010) 316–322.
[3] K.K. Yumkella, P.T. Yillia, Framing the water-energy nexus for the post-2015 development agenda, Aquat. Procedia 5 (2015) 8–12.
[4] J.K. Edzwald, Dissolved air flotation and me, Water Res. 44(7) (2010) 2077–2106.
[5] M. Karhu, T. Leiviskä, J. Tanskanen, Enhanced DAF in breaking up oil-in-water emulsions, Sep. Purif. Technol. 122 (2014) 231–241.
[6] N.T. Manjunath, I. Mehrotra, R.P. Mathur, Treatment of wastewater from slaughterhouse by DAF-UASB system, Water Res. 34(6) (2000) 1930–1936.
[7] S. Brittle, P. Desai, W.C. Ng, A. Dunbar, R. Howell, V. Tesař, W.B. Zimmerman, Minimising microbubble size through oscillation frequency control, Chem. Eng. Res. Des. 104 (2015) 357–366.
[8] V. Tesař, Mechanisms of fluidic microbubble generation Part I: Growth by multiple conjunctions, Chem. Eng. Sci. 116 (2014) 843–848.
[9] F. Rehman, G.J.D. Medley, H. Bandulasena, W.B.J. Zimmerman, Fluidic oscillator-mediated microbubble generation to provide cost effective mass transfer and mixing efficiency to the wastewater treatment plants, Environ. Res. 137 (2015) 32–39.
[10] V. Martínez-Gómez, R. Pérez-Garibay, J. Rubio, Factors involving the solids-carrying flotation capacity of microbubbles, Miner. Eng. 53 (2013) 160–166.
[11] T. Zheng, Q. Wang, T. Zhang, Z. Shi, Y. Tian, S. Shi, N. Smale, J. Wang, Microbubble enhanced ozonation process for advanced treatment of wastewater produced in acrylic fiber manufacturing industry, J. Hazard. Mater. 287 (2015) 412–420.
[12] S. Liu, Q. Wang, H. Ma, P. Huang, J. Li, T. Kikuchi, Effect of micro-bubbles on coagulation flotation process of dyeing wastewater, Sep. Purif. Technol. 71(3) (2010) 337–346.

[13] L.-B. Chu, X.-H. Xing, A.-F. Yu, X.-L. Sun, B. Jurcik, Enhanced treatment of practical textile wastewater by microbubble ozonation, Process Saf. Environ. Prot. 86 (5) (2008) 389–393.
[14] F. Kobayashi, H. Ikeura, S. Ohsato, T. Goto, M. Tamaki, Disinfection using ozone microbubbles to inactivate *Fusarium oxysporum* f. sp. *melonis* and *Pectobacterium carotovorum* subsp. *carotovorum*, Crop Prot. 30(11) (2011) 1514–1518.
[15] S. Khuntia, S.K. Majumder, P. Ghosh, Quantitative prediction of generation of hydroxyl radicals from ozone microbubbles, Chem. Eng. Res. Des. 98 (2015) 231–239.
[16] L. Henthorne, B. Boysen, State-of-the-art of reverse osmosis desalination pretreatment, Desalination 356 (2015) 129–139.
[17] T. Peters, D. Pintó, E. Pintó, Improved seawater intake and pre-treatment system based on Neodren technology, Desalination 203(1–3) (2007) 134–140.
[18] L.O. Villacorte, S.A.A. Tabatabai, D.M. Anderson, G.L. Amy, J.C. Schippers, M.D. Kennedy, Seawater reverse osmosis desalination and (harmful) algal blooms, Desalination 360 (2015) 61–80.
[19] Y. El Rayess, C. Albasi, P. Bacchin, P. Taillandier, M. Mietton-Peuchot, A. Devatine, Analysis of membrane fouling during cross-flow microfiltration of wine, Innovative Food Sci. Emerg. Technol. 16 (2012) 398–408.
[20] J.M.O. Pulido, A review on the use of membrane technology and fouling control for olive mill wastewater treatment, Sci. Total Environ. (in press), doi: 10.1016/j.scitotenv.2015.09.151.
[21] M. Rahimi, S.S. Madaeni, M. Abolhasani, A.A. Alsairafi, CFD and experimental studies of fouling of a microfiltration membrane, Chem. Eng. Process. Process Intensif. 48(9) (2009) 1405–1413.
[22] S. Chellam, M.A. Sari, Aluminum electrocoagulation as pretreatment during microfiltration of surface water containing NOM: A review of fouling, NOM, DBP, and virus control, J. Hazard. Mater. 304 (2016) 490–501.
[23] K. Chon, J. Cho, S.J. Kim, A. Jang, The role of a combined coagulation and disk filtration process as a pre-treatment to microfiltration and reverse osmosis membranes in a municipal wastewater pilot plant, Chemosphere 117 (2014) 20–26.
[24] H.-C. Kim, In-line coagulation with quaternary amine polymer prior to microfiltration of humic-rich water, J. Colloid Interface Sci. 459 (2015) 151–159.
[25] K. Kimura, K. Tanaka, Y. Watanabe, Microfiltration of different surface waters with/without coagulation: Clear correlations between membrane fouling and hydrophilic biopolymers, Water Res. 49 (2014) 434–443.
[26] J. Park, H.-Y. Kim, P.-K. Park, Split injection of coagulant to enhance the water permeability of a cake layer in a coagulation–microfiltration process, J. Ind. Eng. Chem. 21 (2015) 363–368.
[27] B.K. Pramanik, F.A. Roddick, L. Fan, A comparative study of biological activated carbon, granular activated carbon and coagulation feed pre-treatment for improving microfiltration performance in wastewater reclamation, J. Membr. Sci. 475 (2015) 147–155.
[28] M.A. Sari, S. Chellam, Surface water nanofiltration incorporating (electro) coagulation–microfiltration pretreatment: Fouling control and membrane characterization, J. Membr. Sci. 437 (2013) 249–256.
[29] J. Jung, Y.-J. Kim, Y.-J. Park, S. Lee, D.-H. Kim, Optimization of coagulation conditions for pretreatment of microfiltration process using response surface methodology, Environ. Eng. Res. 20(3) (2015) 223–229.
[30] A. Roy, S. De, Resistance-in-series model for flux decline and optimal conditions of Stevia extract during ultrafiltration using novel CAP-PAN blend membranes, Food Bioprod. Process. 94 (2015) 489–499.
[31] M. Sarioglu, G. Insel, D. Orhon, Dynamic in-series resistance modeling and analysis of a submerged membrane bioreactor using a novel filtration mode, Desalination 285 (2012) 285–294.
[32] S. Lee, P.-K. Park, J.-H. Kim, K.-M. Yeon, C.-H. Lee, Analysis of filtration characteristics in submerged microfiltration for drinking water treatment, Water Res. 42(12) (2008) 3109–3121.
[33] Y.-J. Kim, T. Yun, S. Lee, D. Kim, J. Kim, Accelerated testing for fouling of microfiltration membranes using model foulants, Desalination 343 (2014) 113–119.